Draft: December 18, 2002

Apolipoprotein A-I's C-terminal domain contains a lipid sensitive conformational trigger

Michael N. Oda[1*], Trudy M. Forte[2], Robert O. Ryan[1], and John C. Voss[3]
[1] Children's Hospital Oakland Research Institute, Oakland, CA 94609-1673
[2] Life Sciences Division MS 1-222, Lawrence Berkeley National Laboratory, Berkeley, CA 94720
[3] Dept. of Biological Chemistry, University of California, Davis, CA 95616

* To whom correspondence should be addressed.
FAX: (510) 450-7920

Phone: (510) 428-3885 ext. 2475
Email: moda@chori.org

Summary

The intrinsic conformational flexibility of exchangeable apolipoproteins allows their existence in lipid-free and lipid-associated states. The C-terminal domain of human apolipoproteinA-I (apoA-I), the major protein of high density lipoprotein (HDL), plays an essential role in its lipid-binding and self-association. Site directed spin label electron paramagnetic resonance spectroscopy was used to examine apoA-I's C-terminal structure in both lipid-free and lipid-associated environments. By positioning a stable free radical spin label at locations throughout the C-terminus, we identified the presence of distinct secondary structural elements. Magnetic interactions of probes localized at positions 163, 217, and 226 in single and double labeled apoA-I provided inter/intra-molecular distance information, serving as the basis for mapping apoA-I tertiary and quaternary structure. Spectra of labeled apoA-I in reconstituted HDL show that lipid induces defined segments of random coil and β-strand to transition to an extended α-helix that presents a continuous hydrophobic surface. The conformational transition of random coil to α-helix may serve as a means to overcome the energy barriers of lipid sequestration, which has significant implications with respect to cholesterol efflux, HDL assembly and cholesterol homeostasis.

Apolipoprotein A-I (apoA-I) is the major protein on high density lipoprotein (HDL) and a primary determinant of HDL structure, composition, and stability. HDL serves a cardioprotective role as the principal mediator of the reverse cholesterol transport pathway, the process whereby excess cholesterol is removed from peripheral tissues and transported to the liver, adrenal gland and steroidogenic organs. Lipid-poor apoA-I interacts with the ATP binding cassette transporter A-1 to accept cell-derived cholesterol and phospholipid, initiating lipoprotein assembly[1,2]. As a structural component of HDL, apoA-I activates the anti-atherogenic enzyme lecithin:cholesterol acyltransferase[3] and associates with the anti-oxidative enzyme paraoxonase[4]. It is also a ligand for scavenger receptor, class B, type 1[5].

A unique and definitive characteristic of apoA-I is its ability to maintain solubility in either lipid-free or lipid-associated states. The predominant secondary structural element present in exchangeable apolipoproteins is the amphipathic α-helix. In the absence of lipid, apoA-I is proposed to organize into a helix bundle that is stabilized by hydrophobic helix-helix interactions. Helix bundle apolipoproteins undergo a conformational change that results in substitution of helix-helix interactions for helix-lipid interactions[6,7]. In the case of apoA-I, the extreme N- and C-terminal regions of this 243 amino acid protein are likely to modulate this function. Deletion of the first 43 amino acids at the N-terminus induces a dramatic conformational change in apoA-I that is proposed to mimic its lipid-associated state[8,9]. X-Ray crystallography of (Δ1-43) apoA-I revealed an extended α-helical, horseshoe shaped molecular

architecture, whose dimensions approximate nascent discoidal apoA-I phospholipid complexes[10].

While the N-terminus of apoA-I is important for maintenance of its lipid-free conformation, the C-terminus mediates apoA-I self-association and lipid-binding. Lipid affinity analysis of the eight tandem 22 amino acid segments of apoA-I identified residues in the C-terminus (220-241) as bearing the greatest lipid binding properties[11], suggesting that this region may draw apoA-I into proximity of biological membranes or lipid complexes. C-terminal deletion mutants (Δ190-243, Δ212-233, and Δ213-243) are significantly impaired in lipid binding ability[12,13]. Similarly, the self-association normally observed for lipid-free apoA-I[14] at concentrations > 0.1 mg ml^{-1} is abrogated by deletion of residues 185-243 or 209-243[15].

Secondary structure of lipid-free apoA-I's C-terminus

Although lipid-free apoA-I's C-terminal domain has been extensively studied, it remains refractory to detailed structural analysis and has been consistently characterized as disordered[8,16]. To investigate the molecular basis underlying the obligatory role of the apoA-I C-terminus in lipid-binding and the effect of lipid association on apoA-I structure, we employed site directed spin label electron paramagnetic resonance spectroscopy (SDSL-EPR). Thirty-nine unique human apoA-I variants possessing a single cysteine substitution at specified locations between residues 163 to 243 were labeled with methanethiosulfonate spin label (MTS; Fig. 1*a*, Inset) and subjected to SDSL-EPR analysis. The spectra reveal diversity in structural order (Fig.

1*a*), with line shapes ranging from very sharp reflecting a disordered backbone; to very broad, reflecting sites constrained by tertiary contacts. Over the length of this eighty-residue sequence, unique segments of secondary structure were identified.

The first distinct region identified by SDSL-EPR analysis encompasses residues 163 to 185. Spin-label probes incorporated into this portion of the molecule display dynamics consistent with an ordered secondary structure. Broad line shapes observed with the label at positions 163, 167, 170, 178 and 185 indicate strong side chain immobilization. When projected on a helical wheel diagram, these residues align on the hydrophobic face of an amphipathic α-helix (Fig. 1*b*), defining a site of intra- or inter-molecular contact. The opposing face of this α-helix is interspersed with charged residues. The surface propensity of the polar face of this helix is confirmed by the greater motional freedom of spin label moieties located at positions 173, 176, 180, and 183 (Fig. 1*a*,*b*).

Spin labels positioned at residues 188, 190, 193, 195, 198, 200, 202, and 205 identify a second distinct structural region, characterized by very sharp lines (Fig. 1*a*). These spectra report not only a lack of tertiary contact but also a lack of an ordered backbone, indicative of a flexible, loop-like region. This random coil-like segment is followed by a third distinct structural region, as revealed by EPR spectra of apoA-I harboring spin-labeled side chains at positions between residues 208 to 219. Within this latter sequence, there is a striking contrast between the EPR spectra of odd and even numbered positions, wherein odd numbered positions display a significant fraction of strongly immobilized side chains (Fig. 1*a*,*c*). This type of asymmetry is consistent with a

periodic change in side chain orientation imposed by the backbone of a β-strand conformation wherein the steric environments of the two faces are distinct. This regular pattern ends at position 220, a site occupied by proline in native apoA-I.

Similar to residues 208–219, spectra of lipid-free apoA-I spin-labeled at residues 221–241 display two components, one with a narrow line width and the other with a broad line width. The high mobility displayed by the probe when located at position 238 or 241 contrasts with the immobilized components displayed by positions 221, 226, 232 and 236. These observations agree with an amphipathic α-helical secondary structure for this region, with positions 221, 226, 232 and 236 aligned on the hydrophobic face. Fig. 1*d* depicts a linear map of secondary structure elements in the C-terminal third of lipid-free apoA-I.

Sites of quaternary contact

Because of the C-terminal domain's essential role in lipid-free apoA-I self-association, we evaluated EPR spectra for evidence of spin coupling. Since each apoA-I contains a single label moiety, spin-coupling interactions can only occur inter-molecularly between proximally positioned (4 – 22 Å) nitroxide labels of paired apoA-I. Of the positions examined, only four (163, 217, 226, and to a lesser extent, 167) displayed a level of spectral broadening that suggests the presence of spin-coupling interactions (Fig. 2*a*). The highly broadened spectra observed with a nitroxide radical bound at positions 163, 217, or 226 indicates distance-dependent dipolar interactions between two or more labels on separate polypeptides. Confirmation of the existence of

such interactions is seen by the nonionic detergent (empigen) induced increase in spectral line intensities of probes located at positions 163, 217, and 226. Line intensities for probes without spin-coupling interactions (positions 176 or 209) are unaffected by empigen (Fig. 2*a*). Spectral broadening is unaffected by dilution of apoA-I to 0.5 mg/ml (apoA-I is predominantly dimeric at this concentration), suggesting that the dipolar coupling observed is specific to the apoA-I dimer.

Tertiary alignment of C-terminal secondary structures

The above observations are consistent with an anti-parallel interaction involving the C-termini of paired apoA-I molecules. The geometric constraints of such an interaction predict that residues 163, 217 and 226 are proximal within the apoA-I monomer. ApoA-I bearing spin-label moieties at positions 163/217 and 163/226 were combined with unlabeled WT apoA-I in a ratio of 1:4 (labeled:unlabeled apoA-I), minimizing the contribution of inter-molecular magnetic interactions to the dipolar coupling measurements. When spectra from these double labeled apoA-I are compared to the composite sum spectra of their single labeled counterpart (also combined with unlabeled apoA-I; Fig. 2*b*), it is apparent that intra-molecular dipolar coupling is present. As in the single label experiment, the addition of empigen induced increases in spectral line intensities to levels equivalent the composite spectra (data not shown). When considered within the context of the observed secondary structure, we conclude that residues 163, 217, and 226 cluster within the apoA-I monomer (Fig. 2*c*) and the region between residues 188 and 205 exists as a flexible loop.

Lipid-induced conformational changes

To evaluate dynamic inter-conversions of the C-terminal region of apoA-I upon interaction with lipid, a series of spin labeled apoA-I molecules were examined in the lipid-associated state. Isolated reconstituted HDL particles were subjected to EPR analysis and compared to corresponding spectra of spin labeled lipid-free apoA-I (Fig. 3*a*). In the lipid-bound state all spectra examined were consistent with an ordered secondary structure. In certain cases, the spectra converted from two-state (bearing both a narrow line width and broad line width component) to single-state homogeneous spectra (e.g. residues 212 and 235).

Since probe mobility depends on the order of the backbone and the physical environment surrounding the side chain, analysis of side chain dynamics serves as a simple yet powerful method to elucidate a protein's structural topography[17]. The asymmetric arrangement of a region of secondary structure with respect to environment (e.g. solvent or protein contacts) is revealed in the modulation of the inverse of the central line width (δ^{-1}) as a function of sequence position. Comparing the δ^{-1} values for lipid-free (Fig. 3*b*) and lipid-bound (Fig. 3*c*) apoA-I, it is clear that residues in the loop region (188–205) undergo the most dramatic change upon lipidation. The δ^{-1} values for lipid-free residues in this region are greater than 0.4. Following lipidation there is a general increase in the order of this region, with all δ^{-1} values measuring less than 0.4. Furthermore, modulation of δ^{-1} in the lipid-bound samples correlates well to a single span of α-helical structure from 183 to 236 consistent with X-ray crystallography

data[10]. Finally, none of the spin-labeled positions examined display evidence of dipolar interactions in the lipid-associated state.

These data support a model wherein apoA-I adopts an extended α-helix conformation that presents a roughly continuous hydrophobic surface (Fig. 4*a*). Conversion of the β-sheet segment to α-helix will disrupt the dimer interface, promoting lipidation. Considering that the random coil loop centered at residue 200 also reconfigures to α-helix during lipidation, the overall structure of apoA-I apparently converts from a compact hydrophobically shielded conformation (Fig. 4*a*, left) to an elongated hydrophobically exposed state. Such a structure is well suited to circumscribe the periphery of nascent HDL particles, akin to the "belt" model proposed by Borhani et al.[10].

Viral fusion proteins – conformational analogue

The lipid-triggered conformational switch in the apoA-I C-terminus has parallels in the pH dependent structural transition of hemagglutinin (HA) viral fusion protein[18]. HA undergoes a conformational transition in which a random coil domain 36-residues long is converted to α-helix, extending the protein by 100Å into an elongated membrane fusion-competent conformation in what has been termed a "spring-loaded" trigger mechanism induced by low pH[19] (Fig. 4*b*). Similar to viral fusion proteins, the random coil to α-helix transition in apoA-I's C-terminus acts as a lipid-sensitive trigger and likely contributes to the energetics of apoA-I lipidation[20,21]. This enthalpic contribution

to the free energy of lipid-association would not be available to proteins already assuming an α-helical conformation.

Conclusions

In summary, our observations demonstrate the power of SDSL-EPR in discriminating the conformation and dynamics of exchangeable apolipoproteins as a function of reversible lipid-binding interactions that have profound effects on plasma lipid homeostasis. This application of EPR has provided insight into the structure of apoA-I in two distinct environments, presenting a molecular basis for apoA-I self-association and lipid binding-induced conformational adaptations. These results have led us to conjecture that the functional necessity of the apoA-I C-terminus may not only be to serve as a site of initial lipid contact but also as a source of energy to drive the process of lipid association. Because of the presence of random coil segments in many exchangeable apolipoproteins and their observed lipid induced transition to α-helix, the conformational transition observed here may represent a mechanism common to exchangeable apolipoproteins.

Methods

Mutation synthesis. Cys substitution mutations within apoA-I cDNA (L163C-N241C) were created using either primer directed PCR mutagenesis or by the Mega-Primer PCR method[22]. The mutations were verified by dideoxy automated fluorescent sequencing.

Protein preparation. Human apoA-I expression and purification was carried out as described[23,24]. Phospholipid analysis performed on the purified protein confirmed the absence of lipid.

Site directed spin labeling. Spin-labeling was performed on 5 mg of cysteine-substituted apoA-I while bound to a Hi-Trap chelating column. ApoA-I was loaded onto the columns in wash buffer (20 mM $NaPO_4$, 0.5 M NaCl, 3 M guanidine-HCl, pH 7.4) containing 0.25 mM DTT. Reduced cysteines were spin-labeled by the sequential column passage of wash buffer containing 100 µM TCEP and wash buffer containing 120 µM MTS. Free spin-label was removed by passage of wash buffer followed by PBS. The spin-labeled protein was eluted from the column using 20 mM $NaPO_4$, 0.5 M NaCl, 0.5 M Imidazole, pH 7.4 and dialyzed against TBS. Fourier Transform infrared spectroscopy was performed on select spin-labeled apoA-I samples to confirm global folding of the molecule was unaffected by the presence of the spin label, as determined by secondary structure content.

ApoA-I lipidation. Discoidal HDL were prepared by a modified method originally described by Nichols et al.[25]. Equal volumes of 22 mM sodium cholate in TBS and 16.3 mM palmitoyl-oleoyl phosphatidylcholine in TBS were combined and vortexed. The mixture was incubated at 37° C until clear. Three mg spin labeled apoA-I was added to

the cleared dispersion and incubated 1 h at 37° C. Cholate was removed by dialysis against TBS. HDL were isolated by density gradient centrifugation. Samples containing both protein and lipid were pooled. The size of lipidated discoidal complexes was confirmed by gradient gel electrophoresis[25].

EPR spectroscopy. EPR measurements were performed in a JEOL X-band spectrometer fitted with a loop-gap resonator[26,27]. An aliquot of purified, spin-labeled protein (10 μL) at a final concentration of ~5 mg ml^{-1} protein in TBS was placed in a sealed quartz capillary contained in the resonator. Spectra of samples were obtained by a single 60 second scan over 100G at a microwave power of 2 mW and a modulation amplitude optimized to the natural line width (1.5 - 2.5 G) at room temperature (20 – 22° C), as described previously[28]. Double labeled apoA-I and their single labeled counterparts were combined with unlabeled WT apoA-I in a ratio of 1:4 prior to EPR spectroscopy. These samples were examined over a 200G range but otherwise identically to the other samples.

References

1. Bodzioch M. *et al. Nat. Genet.* **22**, 347 (1999).
2. Lawn R.M. *et al. J. Clin. Invest.* **104**, R25 (1999).
3. Fielding, C.J., Shore V.G. & Fielding, P.E. *Biochim. Biophys. Acta* **270**, 513 (1972).
4. Gan, K.N., Smolen, A., Eckerson, H.W. & La Du, B.N. *Drug Metab. Dispos.* **19**, 100 (1991).
5. Xu, S., Laccotripe, M., Huang, X., Rigotti, A., Zannis, V.I. & Krieger, M. *J. Lipid Res.*

38, 1289-98 (1997).

6. Narayanaswami, V. & Ryan, R.O. *Biochim. Biophys. Acta.* **1483**, 15-36 (2000).
7. Wang, J., Sykes, B.D. & Ryan, R.O. *Proc. Natl. Acad. Sci. U S A* **99**, 1188-93 (2002).
8. Roberts, L.M., Ray, M.J., Shih, T.W., Hayden, E., Reader, M.M. & Brouillette, C.G. *Biochemistry* **36**, 7615 (1997).
9. Rogers, D.P., Roberts, L.M., Lebowitz, J., Engler, J.A. & Brouillette, C.G. *Biochemistry* **37**, 945 (1998).
10. Borhani, D.W., Rogers, D.P., Engler, J.A. & Brouillette, C.G. *Proc. Natl. Acad. Sci. U S A* **94**, 12291 (1997).
11. Palgunachari, M.N. *et al. Arterioscler. Thromb. Vasc. Biol.* **16**, 328 (1996).
12. Holvoet, P. *et al. Biochemistry* **34**, 13334 (1995).
13. Minnich, A. *et al. J. Biol. Chem.* **267**, 16553 (1992).
14. Vitello, L.B. & Scanu, A.M. *J. Biol. Chem.* **251**, 1131 (1976).
15. Laccotripe, M., Makrides, S.C., Jonas, A. & Zannis, V.I. *J. Biol. Chem.* **272**, 17511 (1997).
16. Davidson, W.S., Hazlett,T., Mantulin, W.W. & Jonas, A. *Proc. Natl. Acad. Sci. U S A* **93**, 13605 (1996).
17. Hubbell, W.L., Cafiso, D.S. & Altenbach, C. *Nat. Struct. Biol.* **7**, 735-9 (2000).
18. Wiley, D.C. & Skehel, J.J. *Annu. Rev. Biochem.* **56**, 365 (1987).
19. Carr, C.M. & Kim, P.S. *Cell* **73**, 823-32 (1993).
20. Kozlov, M.M. & Chernomordik, L.V. *Biophys. J.* **75**, 1384-96 (1998).
21. Bentz, J. *Biophys. J.* **78**, 886-900 (2000).

22. Kammann, M., Laufs, J., Schell, J. & Gronenborn, B. *Nucleic Acids Res.* **17**, 5404 (1989).

23. Ryan, R.O., Forte, T.M. & Oda, M.N. *Prot. Exp. and Pur.* In Press, (2002).

24. Oda, M.N., Bielicki, J.K., Berger, T. & Forte, T.M. *Biochemistry* **40**, 1710 (2001).

25. Nichols, A.V., Gong, E.L., Blanche, P.J. & Forte, T.M. *Biochim. Biophys. Acta* **750**, 353 (1983).

26. Froncisz, W. & Hyde, J.S. *J. Magn. Reson.* **47**, 515 (1982).

27. Hubbell, W.L., Froncisz, W. & Hyde, J.S. *Rev. Sci. Instrum.* **58**, 1879 (1987).

28. Chomiki, N., Voss, J.C. & Warden, C.H. *Eur. J. Biochem.* **268**, 903-13 (2001).

29. Segrest, J.P. *et al. J. Biol. Chem.* **274**, 31755-8 (1999).

30. Wilson, I.A., Skehel, J.J. & Wiley, D.C. *Nature* **289**, 366-73 (1981).

31. Bullough, P.A., Hughson, F.M., Treharne, A.C., Ruigrok, R.W., Skehel, J.J. & Wiley, D.C. *J. Mol. Biol.* **236**, 1262-5 (1994).

Acknowledgments

We wish to thank Dr. John Crowe, Christine Fang, Barbara-Jean Nitta, and Catherine Robertson for their valuable technical assistance.

Figure Legends

Fig. 1 Secondary structure analysis of lipid-free apoA-I residues 163-241. ***a***, Lipid-free EPR spectra from 39 apoA-I residues (163-241) spin labeled with the thiol-specific MTS (inset). Restrictions in backbone motion imposed by secondary structure are illustrated by differences in the sharpness and symmetry of spectra (eg., residue 202 versus residue 167). The restriction of side chain motion imposed by tertiary contacts is observed by the appearance of broad splittings of the hyperfine extrema in the EPR spectra (red arrows; residue 170 spectra). Spectra consisting of two components are observed for residues containing both a narrow line width (reflecting a highly mobile population; 221 spectra, green dashed line) and a broader line width arising from spin labels attached to a more ordered population (residue 221 spectra, blue dashed line). ***b***, Helical wheel projection of apoA-I residues 163-185. EPR spectra of hydrophobic residues (dark grey) in this region are highly immobilized (blue circles), consistent with a model positioning these residues on an α-helical face directed away from solvent. Charged/polar residues (pink) elicit EPR spectra exhibiting highly mobile side-chain dynamics (red triangles), consistent with a solvent exposed α-helical face. ***c***, Plot of the ratio of ordered to disordered side chains in the region of 209-221. The ratio of the strongly immobilized component intensity (inset; S) to the weakly immobilized component intensity (inset; W) is plotted versus residue position. The amino acids in this region demonstrate a signature periodicity in solvent accessibility, with an alternating maxima/minima, consistent with a β-sheet secondary structure. ***d***, Linear model of lipid-free apoA-I's C-

terminal secondary structure. Shown here is the more ordered conformation of the apoA-I C-terminus.

Fig. 2 Tertiary arrangement of apoA-I secondary structures. ***a***, Dipolar coupling within lipid-free apoA-I dimers. Three positions (163, 217, and 226; blue line) display a level of broadening that suggests dipolar coupling. This is exemplified by the effect of empigen detergent (0.1%; red line). Control spin labeled positions 176 and 209, which exhibit no dipolar coupling, are relatively unaffected by empigen. ***b***, Dipolar coupling within lipid-free apoA-I monomers. Double labeled mutants (163/217 and 163/226; blue line; 200G scan) exhibit dipolar coupling in comparison to the composite sum spectra of their single labeled counterparts (163, 217, and 226; purple line). ***c***, Model for the tertiary arrangement of lipid-free apoA-I's C-terminal domain. The tertiary arrangement of secondary structures in Fig. 1*d* are configured to align residues L163, G217, and K226 (indicated in red) on the same plane and face.

Fig. 3 Comparison of lipid-free and lipid-bound apoA-I structure. ***a***, EPR spectra of reconstituted HDL discs consisting of spin-labeled apoA-I. A consistent feature of lipid-bound apoA-I spectra (red line) is their high degree of uniformity versus the corresponding lipid-free spectra (blue line). Nearly all lipid-bound spectra bear the signature line shape of an ordered α-helical secondary structure. The inverse of the central line width (***c***, inset; δ^{-1}) is plotted as a function of sequence position for lipid-free (39 positions) ***b***, and lipid-bound (13 positions) ***c***, apoA-I to evaluate the effect of

lipidation on the C-terminal domain's secondary structure composition. The modulation of δ^{-1} is dictated by the periodicity of the secondary structure[17]. The modulation of δ^{-1} for the lipid-bound samples correlates well with a simulated plot for an α-helix (cosine function with 3.67 periodicity; ***c***; red line).

Fig. 4. Lipid induced conformational transition of apoA-I and influenza hemagglutinin's fusogenic subunit HA2. ***a***, ApoA-I's lipid-induced structural transition from a compact lipid-free conformation (green) to an extended α-helix (yellow). Although not indicated by the EPR data, lipid-bound apoA-I's extended α-helix (residues 163-243) is modeled bearing a degree of curvature to accommodate the geometric constraints of discoidal HDL[29]. The amphipathic nature of the lipid-bound conformation is indicated by hydrophobic residues (green) and charged residues (purple). ***b***, N-terminal domain of influenza hemagglutinin's fusogenic subunit HA2 at physiological pH[30] (green) and at low pH[31] (yellow; only HA2 is shown).

Figure 1 - Oda *et al.*

Figure 2 - Oda *et al.*

Figure 3 - Oda *et al.*

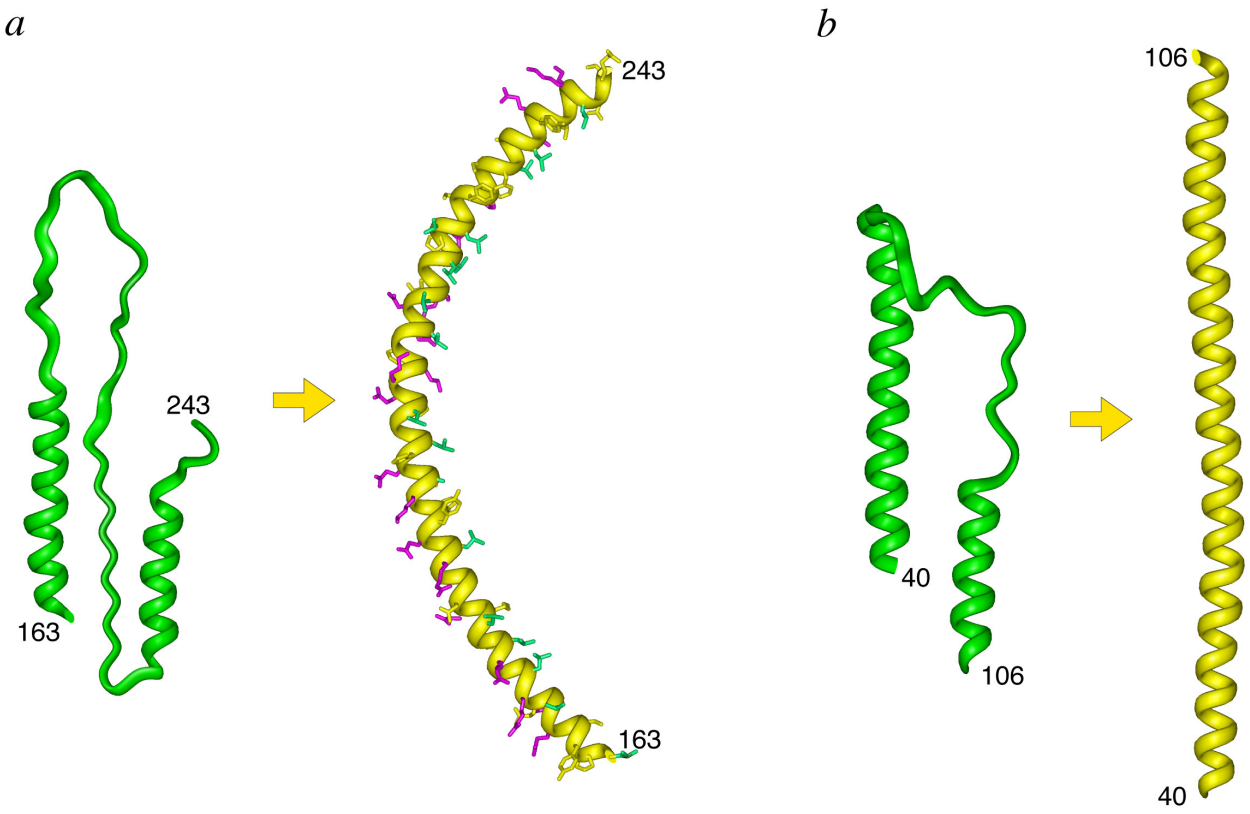

Figure 4 - Oda *et al.*